The EMBO Journal (2011) 30, 524–532 | © 2011 European Molecular Biology Organization | All Rights Reserved 0261-4189/11
www.embojournal.org

THE EMBO JOURNAL

miR-605 joins p53 network to form a p53:*miR-605*:Mdm2 positive feedback loop in response to stress

Jiening Xiao[1,3,4,*], Huixian Lin[1,3,4], Xiaobin Luo[1,2], Xiaoyan Luo[1,2] and Zhiguo Wang[1,2,*]

[1]Research Center, Montreal Heart Institute, Montreal, Canada and [2]Department of Medicine, University of Montreal, Montreal, Canada

In cancers with wild-type (WT) p53 status, the function of p53 is inhibited through direct interaction with Mdm2 oncoprotein, a negative feedback loop to limit the function of p53. In response to cellular stress, p53 escapes the p53:Mdm2 negative feedback to accumulate rapidly to induce cell cycle arrest and apoptosis. We demonstrate herein that an microRNA *miR-605* is a new component in the p53 gene network, being transcriptionally activated by p53 and post-transcriptionally repressing Mdm2. Activation of p53 upregulated *miR-605* via interacting with the promoter region of the gene. Overexpression of *miR-605* directly decreased Mdm2 expression at the post-transcriptional level but indirectly increased the transcriptional activity of p53 on *miR-34a* via downregulating Mdm2; knockdown of *miR-605* did the opposite. Mdm2 inhibitor upregulated expression of both *miR-34a* and *miR-605*, which was mitigated by p53 inhibitor. *miR-605* preferentially induced apoptosis in WT p53-expressing cells, an effect abolished by p53 inhibition. These results indicate that *miR-605* acts to interrupt p53:Mdm2 interaction to create a positive feedback loop aiding rapid accumulation of p53 to facilitate its function in response to stress.

The EMBO Journal (2011) **30,** 524–532. doi:10.1038/emboj.2010.347; Published online 7 January 2011
Subject Categories: chromatin & transcription; RNA
Keywords: apoptosis; gene expression; Mdm2; miRNA; p53

Introduction

In ~50% of human cancers, the gene (TP53) encoding p53 protein, a DNA damage responsive transcription factor that affects diverse cellular processes including transcription, DNA synthesis and repair, cell cycle arrest, senescence and apoptosis, is mutated rendering its tumour suppressor activity inactivated. In the remaining cancers with wild-type (WT) p53 status, its function is inhibited through direct interaction with the human murine double minute 2 (Mdm2) oncoprotein; p53 activates the transcription of Mdm2, which in turns targets p53 for degradation and transcription repression, therefore creating a negative feedback loop to limit the function of p53. Mdm2 is often present at high levels in tumours with WT p53. This autoregulatory feedback loop constitutes the core module of a network of regulatory interactions activated under cellular stresses including DNA damage, hypoxia and oncogene activation. In normal cells, the activity of p53 proteins is kept low by Mdm2, that is Mdm2 negatively regulates the stability of p53 and the transcription of TP53 (Momand *et al*, 1992; Haupt *et al*, 1997; Kubbutat *et al*, 1997; Eischen and Lozano, 2009). In the case of DNA damage, p53:Mdm2 interaction is weakened that allows rapid activation of the p53-mediated pathways leading to cell cycle arrest or apoptosis in case of excessive damage (Barak *et al*, 1993; Harris and Levine, 2005). Blocking the p53:Mdm2 interaction to reactivate the p53 function is a promising anti-cancer strategy. However, recent findings have shown this network to be more complex than previously envisioned and our current understanding of this network is incomplete. In particular, it remained vague how p53 can escape the p53:Mdm2 negative feedback loop to accumulate rapidly in the cell in response to stresses. There may be a 'third' player that can operate to break the p53:Mdm2 negative feedback loop. This study was designed to exploit this issue.

*Corresponding authors. Z Wang, Department of Medicine, Research Center, Montreal Heart Institute, 5000 Belanger East, Montreal, Quebec, Canada H1T 1C8. Tel.: +1 514 376 3330/Ext. 3517; Fax: +1 514 376 1355; E-mails: wangz@mirna-tech.com or zhiguo.wang@icm-mhi.org or J Xiao, Research Center, Montreal Heart Institute, Montreal, Canada PQ H1T 1C8. Tel.: +1 514 376 3330/Ext. 3470; Fax: +1 514 376 1355; E-mail: jieningxiao@yahoo.com
[3]These authors contributed equally to this work
[4]These authors are currently holding positions as full professors in the School of Life Sciences, Guangzhou University, Guangzhou, China

Received: 5 March 2010; accepted: 3 December 2010; published online: 7 January 2011

Results and discussion

Mdm2 as a target of miR-605 for post-transcriptional repression

Recent studies have identified an miRNA *miR-34* as a direct transcriptional target of p53 (He *et al*, 2007; Raver-Shapira *et al*, 2007; Tarasov *et al*, 2007), indicating important participation of miRNAs in the p53 gene network. In an initial effort to explore the potential role of miRNAs in regulating the p53:Mdm2 negative feedback loop, we studied *miR-34* (including *miR-34a*, *miR-34b* and *miR-34c*). However, our computational analysis and experimental results excluded the role of *miR-34* in targeting p53 and Mdm2, consistent with the view that *miR-34* acts as a downstream component mediating the function of p53 (He *et al*, 2007; Raver-Shapira *et al*, 2007; Tarasov *et al*, 2007).

With theoretical prediction of miRNA target genes and of putative *cis*-acting elements for transcription regulation of miRNA genes (Supplementary data), we identified *miR-605* as a top-priority miRNA for our study for it has multiple potential binding sites (12) in the 3′UTR of *Mdm2* mRNA (Supplementary Figure S1) and the promoter region of its host gene PRKG1 contains two high-scored p53 consensus binding

sites (half-sites) within 1125 bp upstream its transcription start site (Supplementary Figure S2; The precursor sequence of *miR-605* is located within the intron 2 of PRKG1 at the genomic location of 52 729 339–52 729 421[+] in the chromosome 10) (Lee *et al*, 2009). These analyses suggest a possibility of *miR-605* to regulate Mdm2 expression at the post-transcriptional level on one hand and to be regulated in its own expression at the transcriptional level by p53 on the other hand.

We set up to examine our hypothesis using the following approaches. We first studied the interactions between *miR-605* and Mdm2 by luciferase reporter gene assay. Transfection of synthetic mature *miR-605* produced ~75% reduction of the luciferase activity of the pMIR-REPORT^{TM} luciferase vector carrying the 3′UTR of Mdm2 to replace that of the luciferase gene in A549 human lung cancer cells that express a low level of endogenous *miR-605* (Figure 1A; Supplementary Figure S3). And this effect was effectively reversed by co-transfection with its antisense oligoribonucleotides (AMO-605). Additionally, application of AMO-605 alone in MCF-7 human breast cancer cells that express a higher level of authentic *miR-605* (MCF-7:A549 = 14:1; Supplementary Figure S3) enhanced the luciferase activity, indicating the tonic repression of the luciferase gene expression by endogenous *miR-605*. The repressive effect of *miR-605* was then confirmed at the protein level using western blot analysis; *miR-605* decreased the protein level of Mdm2 by ~80% in A549 cells (Figure 1B). Similar results were observed in MCF-7 cells (Supplementary Figure S4). Moreover, AMO-605 alone was able to increase the protein level of Mdm2 in MCF-7 cells, presumably by knocking down the endogenous *miR-605* in these cells. Quantitative real-time RT–PCR (qPCR) analyses revealed that Mdm2 mRNA level changed in the opposite direction: transfection of *miR-605* caused ~30% upregulation of Mdm2 mRNA (Figure 1C), which was abolished by co-transfection with AMO-605. This mRNA-increasing effect is likely ascribed to the net outcome between the enhanced p53 activity by *miR-605* (see below) and an *miR-605*-induced degradation process as *miR-605* has a high percentage of complementarity to Mdm2 (Supplementary Figure S1). As negative controls, neither *miR-34a* nor a scrambled miRNA caused any significant changes on luciferase activity, and protein and mRNA levels of Mdm2 (Figure 1A–C). Important to note is that in A549 cells that expressed a low level of endogenous *miR-605*, AMO-605 alone failed to alter Mdm2 expression determined by luciferase assay, western blot and qPCR (Figure 1A–C), whereas in MCF-7 cells that express a higher level of *miR-605*, AMO-605 was able to produce derepression of Mdm2.

To obtain confirmative evidence for that the effects observed above are ascribed to the specific interaction between *miR-605* and the binding sites for *miR-605* in the 3′UTR of *Mdm2* mRNA, we introduced nucleotide-substitution mutations to 4 out of 12 predicted binding motifs corresponding to the seed site of *miR-605* to disrupt base paring between *miR-605*:*Mdm2*. The binding site S3493 has the highest degree of complementarity among the 12 predicted binding motifs (Supplementary Figure S1), S4028 has a medium degree of complementarity, and S3185 and S5426 have the lowest degrees of complementarity. As expected, among the four sites, the site with the highest degree of complementarity (S3493) conferred the greatest decrease in luciferase activities and mutation of the site (MT S3493) nearly abolished the

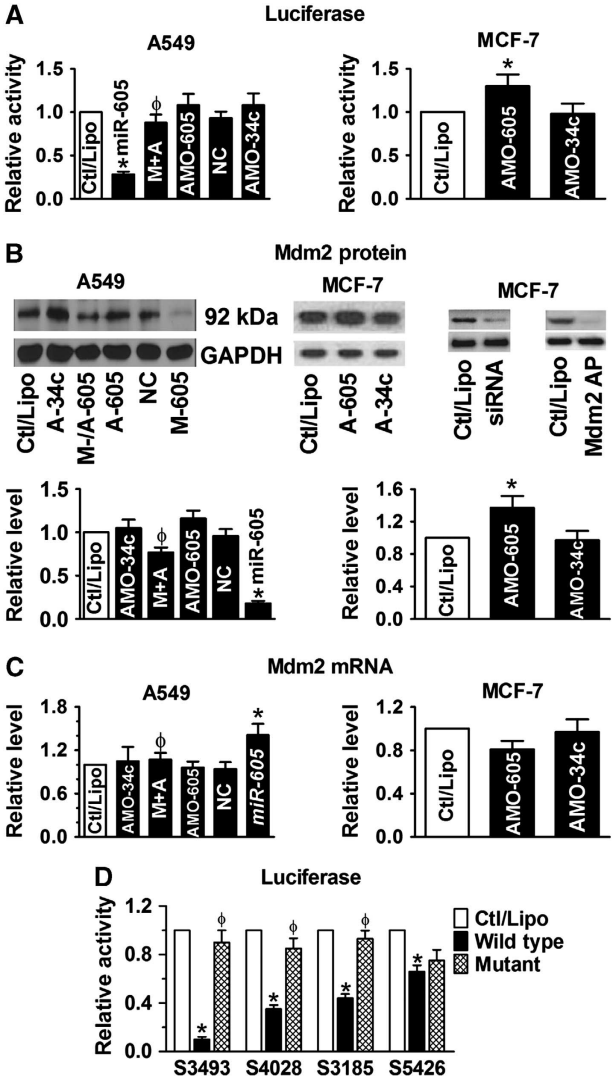

Figure 1 Mdm2 as a target of *miR-605* for post-transcriptional repression. (**A**) Role of *miR-605* in repressing Mdm2, determined by luciferase activity assays with the pMIR-REPORT luciferase miRNA expression reporter vector carrying the 3′UTR of *miR-605* target gene *Mdm2* in A549 (left) and MCF-7 (right) cells. AMO-605 and AMO-34a: antisense nucleotides to *miR-605* and *miR-34a* (used as a control), respectively; M + A: co-transfection of *miR-605* and AMO-605; NC: negative control with scrambled miRNAs. Control cells were mock treated with lipofectamine 2000 (Ctl/Lipo). $^{*}P<0.05$ versus Ctl/Lipo; $^{\Phi}P<0.05$ versus *miR-605* alone; $n=6$ for each group. (**B**) Western blot analysis revealing repression of Mdm2 protein by *miR-605* in A549 cells (left) and in MCF-7 cells (right). M-/A-605: co-transfection of *miR-605* and AMO-605; A-605: AMO-605; A-34a: AMO-34a; M-605: *miR-605*; NC: negative control with scrambled miRNAs; Mdm2 AP: antigenic peptide; siRNA: small interference RNA to Mdm2. $^{*}P<0.05$ versus Ctl/Lipo; $^{\Phi}P<0.05$ versus *miR-605* alone; $n=4$ for each group. (**C**) Effect of *miR-605* on Mdm2 mRNA level in A549 (upper) and MCF-7 (lower). M + A: co-transfection of *miR-605* and AMO-605; NC: negative control with scrambled miRNAs. $^{*}P<0.05$ versus Ctl/Lipo; $^{\Phi}P<0.05$ versus *miR-605* alone; $n=4$ for each group. (**D**) Comparison of the effects of *miR-605* on luciferase activities in A549 cells generated by the pMIR-REPORT vectors each carrying a wild-type or mutated fragment of *Mdm2* 3′UTR that spans a single predicted binding site for *miR-605*. Note the differential strengths of inhibition luciferase activities by *miR-605* among the different fragments and the abolishment or abrogation of the effects with the mutant fragments. S3493 indicates the fragment spanning the predicted binding sites starting at location of 3493 of *Mdm2* mRNA (Supplementary Figure S1); the same meaning applies to other three labels. $^{*}P<0.05$ versus Ctl/Lipo; $^{\Phi}P<0.05$ wild-type versus mutant; $n=3$ for each group.

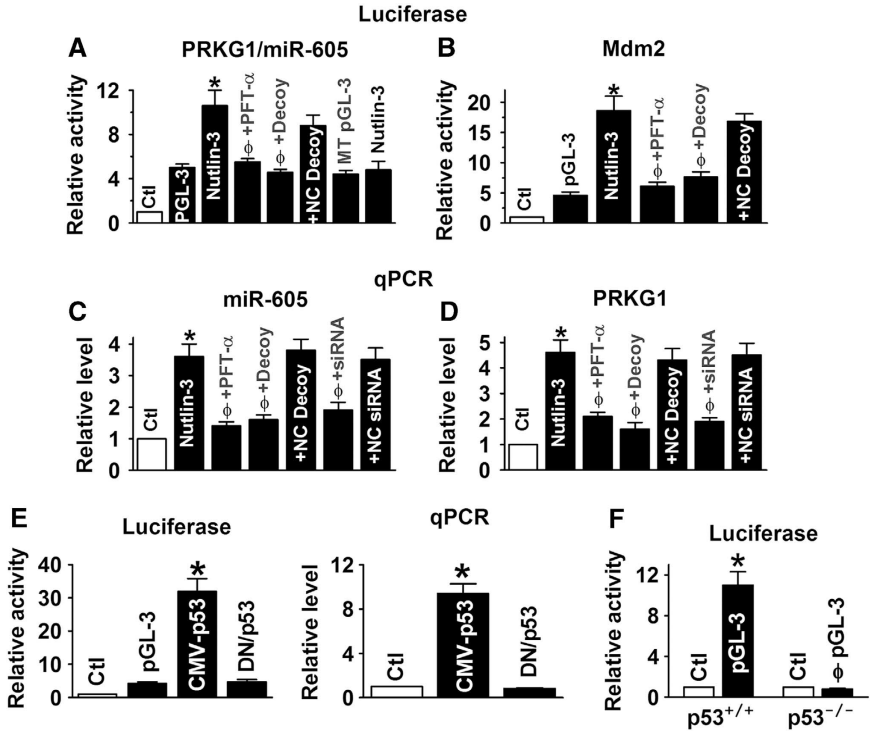

Figure 2 *miR-605* as a target of p53 for transcriptional activation. (**A**) Role of p53 in transactivating the expression of the *miR-605*-host gene PRKG1, assessed by luciferase activity assays with the pGL-3 luciferase reporter vector carrying the promoter region of PRKG1 in MCF-7 cells. Except for control and pGL-3 Base alone, all experiments were preformed in the presence of nutlin-3. Nutlin-3 (1 μM): the Mdm2 inhibitor to activate p53; PFT-α: the p53 inhibitor pifithrin-α (30 μM); Decoy: the decoy oligodeoxyribonucleotide fragment containing a perfect p53-binding site to sequestrate endogenous p53; NC decoy: negative control decoy containing mutated nucleotides in the core region for p53 binding; MT pGL-3: the luciferase reporter vector carrying the mutated p53-binding sites in the promoter region of PRKG1. $^{*}P<0.05$ versus pGL-3 base; $^{\Phi}P<0.05$ versus nutlin-3 alone; $n=4$ for each group. (**B**) Role of p53 in transactivating the expression of the Mdm2 gene, assessed by luciferase activity assays with the pGL-3 luciferase reporter vector carrying the promoter region (the first intron) of Mdm2 in MCF-7 cells. $^{*}P<0.05$ versus pGL-3 base; $^{\Phi}P<0.05$ versus nutlin-3 alone; $n=4$ for each group. (**C**, **D**) Role of p53 in regulating *miR-605* and PRKG1 levels, respectively, evaluated by real-time qRT–PCR in MCF-7 cells. siRNA, small interference RNA to p53; NC siRNA, negative control siRNA. $^{*}P<0.05$ versus pGL-3 base; $^{\Phi}P<0.05$ versus nutlin-3 alone; $n=4$ for each group. (**E**) Luciferase (left) and qPCR (right) evaluation of the effects of p53 overexpression by transient transfection of CMV plasmid carrying wild-type p53 (CMV-p53) in p53-null H1299 cells. The construct carrying the dominant-negative p53 (DN/p53) was used as a control. $^{*}P<0.05$ versus pGL-3 base; $n=4$ for each group. (**F**) Comparison of luciferase activities generated by the pGL-3 luciferase reporter vector carrying the promoter region of PRKG1 between isogenic colorectal carcinoma HCT116 cells ($p53^{+/+}$ and $p53^{-/-}$). $^{*}P<0.05$ versus Ctl; $^{\Phi}P<0.05$ versus $p53^{+/+}$; $n=3$ for each group.

effect of *miR-605* (Figure 1D). By comparison, the other three sites demonstrated weaker effects.

miR-605 as a target of p53 for transcriptional activation

An intronic miRNA is expected to be co-expressed with its host gene. Our experiments indeed confirmed this relationship between *miR-605* and its host gene *PRKG1*. In the first set of experiments, we constructed a pGL-3 luciferase vector by inserting a 2.5-kb fragment spanning the two putative half-sites for p53 upstream the host gene *PRKG1* into the promoter region of the luciferase gene for studying transcription regulation. Treatment with the Mdm2 inhibitor nutlin-3 (1 μM) to activate p53 caused a significant increase in luciferase activity in MCF-7 cells and this effect was abolished by pretreatment with the p53 inhibitor pifithrin-α (PFT-α; 30 μM; Figure 2A). Co-transfection with either p53 decoy oligodeoxyribonucleotide (ODN) to sequestrate p53 (Morishita *et al*, 1997; Gao *et al*, 2006) prevented the nutlin-3-induced luciferase activity, but their respective negative control constructs failed to do so. On the other hand, when the two p53-binding sites were mutated, nutlin-3 failed to affect the luciferase activity. Similar stimulation and silencing of luciferase activities by nutlin-3 and p53 inhibition, respectively, were observed with a *bona fide* p53-responsive promoter—the first intron of the *Mdm2* gene (Figure 2B). Consistent with the above results, nutlin-3 elevated the level of *miR-605* (Figure 2C), along with the upregulation of *PRKG1* mRNA (Figure 2D), which was reversed when co-treated with PFT-α, p53 decoy or siRNA to knockdown p53.

In the second set of experiments, we assessed the ability of p53 overexpression by the CMV plasmid carrying p53 cDNA in the p53-null human lung adenocarcinoma cancer cell line H1299. As shown in Figure 2E, transfection of p53 vector induced a robust increase in PRKG1/*miR-605* promoter activity (left) and *miR-605* level (right), which was not seen with the plasmid carrying the dominant-negative p53.

Next, we compared the luciferase activities between isogenic colorectal carcinoma HCT116 cells ($p53^{+/+}$ and $p53^{-/-}$), and we found substantially higher luciferase activities in $p53^{+/+}$ than in $p53^{-/-}$ HCT116 cells (Figure 2F).

Finally, we verified the physical binding of p53 to the *cis*-elements in the promoter region of the *miR-605* host gene PRKG1 using chromatin immunoprecipitation (ChIP) in conjunction with qPCR semi-quantification (Figure 3A) and

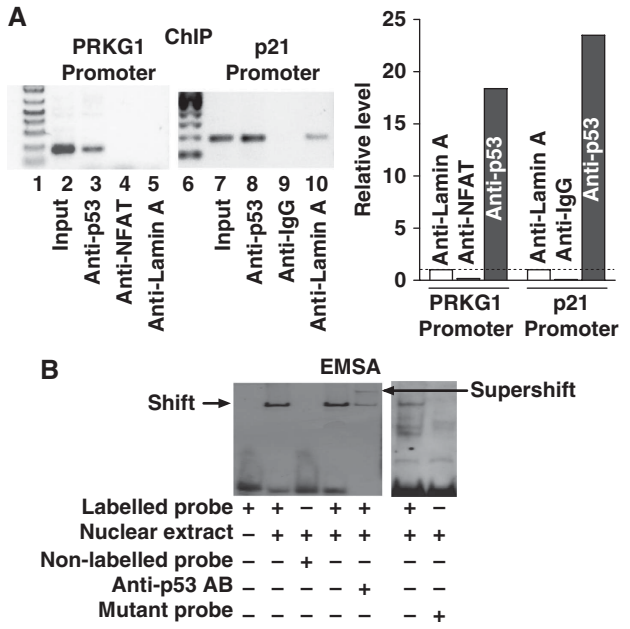

Figure 3 Binding of p53 to the promoter region of the *miR-605* host gene. (**A**) Chromatin immunoprecipitation (ChIP) assay for the presence of p53 on its *cis*-acting elements in the PRKG1 promoter region in MCF-7 cells. p21 promoter region was used as a positive control, NFAT, IgG and lamin A were sued as negative controls. The recovered DNA by anti-p53 to indicate the relative level of p53:PRKG1 or p53:p21 binding was measured by qPCR following ChIP and is expressed as fold changes over anti-lamin A band. Lanes 1 and 6: DNA marker; lane 2: the PCR-amplified band using PRKG1 primer pairs and human genomic DNA without immunoprecipitation; lane 3: the PCR-amplified band using PRKG1 primer pairs and human genomic DNA after p53 antibody immunoprecipitation as a template; lane 4: the PCR-amplified band using PRKG1 primer pairs and human genomic DNA after NFAT antibody immunoprecipitation as a template for negative control; lane 5: the PCR-amplified band using PRKG1 primer pairs and human genomic DNA after lamin-A antibody immunoprecipitation as a template for negative control; lane 7: the PCR-amplified band using p21 primer pairs and human genomic DNA without immunoprecipitation; lane 8: the PCR-amplified band using p21 primer pairs and human genomic DNA after p53 antibody immunoprecipitation as a template for positive control; lane 9: the PCR-amplified band using p21 primer pairs and human genomic DNA after IgG antibody immunoprecipitation as a template for negative control; lane 10: the PCR-amplified band using p21 primer pairs and human genomic DNA after lamin-A antibody immunoprecipitation as a template for negative control. (**B**) Electrophoresis mobility shift assay (EMSA) to indicate the *in vitro* physical binding of p53 to the *cis*-elements in the PRKG1 promoter region using the nuclear extract from MCF-7 cells. A positive control experiment was performed using the p53 decoy containing the canonical p53-binding sites (right panel). Note the shift band representing protein–DNA binding that is abolished with excessive non-labelled probes or with the mutant fragment. Also note the supershift band picked up by the p53 antibody (anti-p53 AB) representing p53–*cis*-elements binding. The probe was a digoxigenin (DIG)-labelled oligonucleotides fragment containing p53-binding site.

electrophoresis mobility shift assay (EMSA) with supershift (Figure 3B), using anti-p53 antibody to indicate the specificity of interactions.

While these above data clearly indicate the transcriptional control of *miR-605* by p53, we sought to clarify whether *miR-605* can produce post-transcriptional influence on p53 gene (*TP53*). Our experiments excluded this possibility by showing that *miR-605* failed to alter the luciferase activity elicited by the pMIR-REPORT vector carrying the 3′UTR of *TP53*

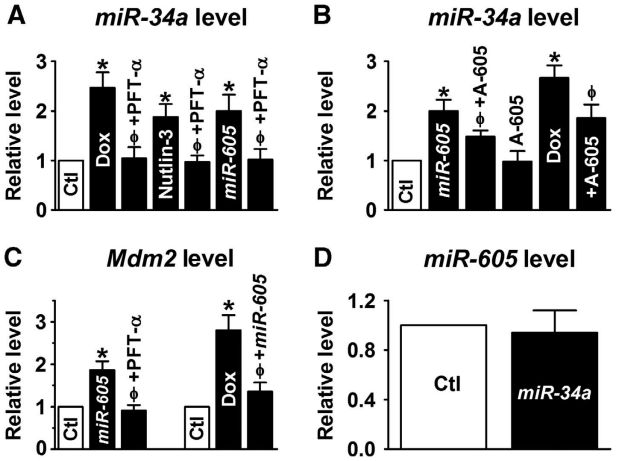

Figure 4 *miR-605* enhances transactivation activity of p53. (**A**, **B**) Regulation of *miR-34a* expression by p53 in MCF-7 cells, determined by real-time RT–PCR. Ctl/Lipo: cells mock-treated with lipofectamine 2000 for control; *miR-605*: cells transfected with *miR-605* (10 nM); + AMO-605 (10 nM): co-transfection of AMO-605 (10 nM) with *miR-605* (10 nM); AMO-605: treatment with AMO-605 alone; A-605: AMO-605; Dox: p53 activator doxorubicin (0.5 μM); PFT-α: p53 inhibitor pifithrin-α (30 μM); Nutlin-3 (1 μM): Mdm2 inhibitor. $^{*}P<0.05$ versus Ctl; $^{\Phi}P<0.05$ versus Dox, Nutlin-3 or *miR-605* alone; $n=5$ for each group. (**C**) Regulation of Mdm2 mRNA level in MCF-7 cells. $^{*}P<0.05$ versus Ctl; $^{\Phi}P<0.05$ versus *miR-605* or Dox; $n=4$ for each group. (**D**) Effects of *miR-34a* on *miR-605* expression in MCF-7 cells ($n=3$ for each group).

(Supplementary Figure S5). This is consistent with the lack of binding sites for *miR-605* in the *TP53* gene. By comparison, *miR-214*, which has its binding site in the 3′UTR of *TP53*, robustly decreased the luciferase activity as expected.

These findings prompted us to deduce that *miR-605* might serve as a regulatory molecule of p53:Mdm2 interaction, being transactivated by p53 on one hand and repressing Mdm2 on the other hand. And joining of *miR-605* is able to switch the p53:Mdm2 negative feedback loop to a positive feedback loop favouring p53 function. If this is true, then we should be able to see the following. First, there is an increase in p53 transcriptional activity while *miR-605* is overexpressed to repress Mdm2. Second, disruption of p53:Mdm2 interaction should be able to upregulate *miR-605* expression. The results from our following experiments indeed support these notions.

miR-605 enhances transactivation activity of p53

Both MCF-7 and A549 cells are known to express WT p53. It was anticipated that by repressing Mdm2, *miR-605* should be able to enhance p53 transcriptional activity. To test this notion, we assessed the effect of p53 activation by doxorubicin (Dox), transfection of *miR-605*, and by inhibition of Mdm2 by nutlin-3 (Vassilev, 2007; Shangary and Wang, 2009) on the expression level of *miR-34a*, an established transcriptional target of p53 (Chang *et al*, 2007; He *et al*, 2007; Raver-Shapira *et al*, 2007; Tarasov *et al*, 2007; Welch *et al*, 2007). As shown in Figure 4A, these manoeuvers all increased *miR34a* transcript and strikingly, their effects were all antagonized by the inhibitor of p53 (PFT-α). Further, the effect of *miR-605* was also reversed by AMO-605 (Figure 4B). Moreover, application of AMO-605 alone did not significantly alter *miR-34a* level, but in the presence of Dox this treatment reduced *miR-34a* level (Figure 4B).

Increase in p53 transcriptional activity by *miR-605* was further evidenced by elevated mRNA levels of p53 target gene p21/CDKN1A (Supplementary Figure S6A). The results suggest that the upregulation of *miR-34a* induced by *miR-605*, as well as by p53 activation strategies (by DNA-damaging agent and Mdm2 inhibition), was mediated by p53. In other words, *miR-605* acts through enhancing p53 activity; without p53 activation, *miR-605* was unable to influence *miR-34a* expression. *miR-605* did not significantly change p53 protein level, neither did nutlin-3 in MCF-7 cells 48 h after the treatments (Supplementary Figure S6B). However, when measured 24 h after treatment with nutlin-3 or *miR-605* upregulation of p53 proton levels were observed in $p53^{+/+}$ HCT116 (Supplementary Figure S6C), possibly due to reduced E3 ubiquitin ligase activity of Mdm2 (Haupt *et al*, 1997; Honda *et al*, 1997).

We have shown in Figure 1C that *miR-605* increased the transcript level of Mdm2. To see whether this was attributable to the enhancement of p53 activity, we pretreated MCF-7 cells with PFT-α before *miR-605* transfection. As depicted in Figure 4C, without PFT-α, *miR-605* was able to elevate Mdm2 mRNA level as expected, but in the presence of PFT-α, *miR-605* lost the ability to do so. On the other hand, cells incubated with Dox demonstrated increased transcription of Mdm2, but pretreatment with AMO-605 abrogated the effect (Figure 4C).

While we have shown that *miR-605* was able to upregulate *miR-34a* (Figure 4A), we found that *miR-34a* failed to alter expression of *miR-605* (Figure 4D), consistent with the view that *miR-34a* does not target p53 (Chang *et al*, 2007; He *et al*, 2007; Raver-Shapira *et al*, 2007; Tarasov *et al*, 2007; Welch *et al*, 2007) nor Mdm2.

Implication of miR-605 participation in the p53:Mdm2 signalling pathway

In order to see whether the participation of *miR-605* in the p53 gene network can be translated into corresponding cellular functions, we carried out the following experiments. We first demonstrated that like Dox or nutlin-3, *miR-605* preferentially induced apoptotic cell death in $p53^{+/+}$ over $p53^{-/-}$ HCT116 cells (Figure 5A and B). Intriguingly, co-transfection of AMO-605 only partially reversed, whereas treatment of PFT-α was able to abolish, the apoptosis promoting of *miR-605* (Figure 5A and B, left panels) in $p53^{+/+}$ HCT116 cells, despite that AMO-605 was able to completely wipe out *miR-605* (Supplementary Figure S7). Further, pretreatment with AMO-605 alone to knockdown endogenous *miR-605* rendered a significantly less extent of apoptosis induced by either Dox or nutlin-3 (Figure 5A and B, right panels). Strikingly, AMO-34a prevented the apoptosis-promoting effect of *miR-605* more efficiently than AMO-605 though it had no effect on *miR-605* level (Figure 5C; Supplementary Figure S7). By comparison, $p53^{-/-}$ HCT116 cells did not respond to *miR-605*. On the other hand, AMO-605 failed to affect the apoptotic effect of *miR-34a*, neither did PFT-α (Figure 5C). The apoptotic cell death was further verified by measurement of caspase-3 activities (Figure 5D). We subsequently confirmed that in response to p53 activation by nutlin-3, *miR-605* level was significantly upregulated only in $p53^{+/+}$ HCT116 cells, and so was *miR-34a* level (Figure 5E), further verifying that both of these two miRNAs are target genes of p53 for transcriptional regulation.

Qualitatively, the same effects of *miR-605* on apoptosis were also observed in WT p53-expressing MCF-7 cells than of p53-null human breast cancer MDA-MB-436 cells (Lacroix and Leclercq, 2004; Keimling and Wiesmüller, 2009) (Supplementary Figure S8).

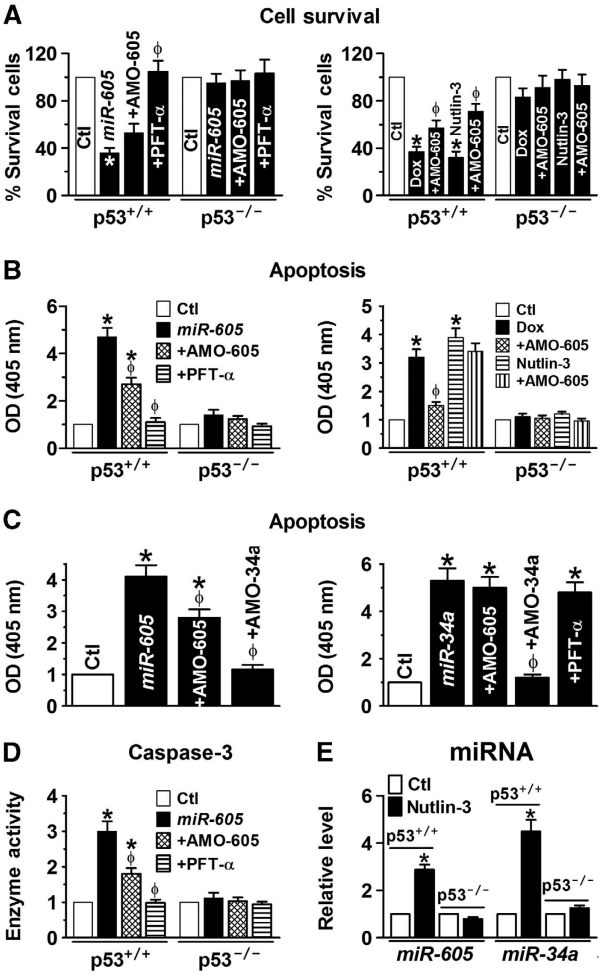

Figure 5 Role of *miR-605* in regulating cell survival and apoptosis. (**A**) Effects of *miR-605* on cell viability in isogenic colorectal carcinoma HCT116 cells ($p53^{+/+}$ and $p53^{-/-}$), as determined by MTT methods. Note that AMO-605 only partially reversed the inhibitory effects of *miR-605* (left panel) and of Dox (0.5 μM) or Nutlin-3 (3 μM; right panel) on cell survival; whereas PFT-α completely reversed the effects. *miR-605* and Dox failed to produce any significant effect in $p53^{-/-}$ HCT116 cells. Ctl: cells mock-treated with lipofectamine 2000; + AMO-605: co-transfection of AMO-605 and *miR-605*; AMO-605: transfection of AMO-605 alone; + PFT-α: application of PFT-α after transfection with *miR-605*. $^{*}P<0.05$ versus Ctl; $^{\Phi}P<0.05$ versus *miR-605* or Dox or Nutlin-3 alone; $n=4$ for each group. (**B**) Effects of *miR-605* on apoptotic cell death in $p53^{+/+}$ and $p53^{-/-}$ HCT116 cells, as determined by optical density (OD at 405 nm) obtained by ELISA. $^{*}P<0.05$ versus Ctl; $^{\Phi}P<0.05$ versus *miR-605* or Dox or Nutlin-3 alone; $n=4$ for each group. (**C**) Effects of AMO-605 and AMO-34a on apoptosis induced by *miR-605* (left panel) and *miR-34a* (right panel) in $p53^{+/+}$ HCT116 cells. $^{*}P<0.05$ versus Ctl; $^{\Phi}P<0.05$ versus *miR-605* or *miR-34a* alone; $n=4$ for each group. (**D**) Mean OD values ($n=4$) indicating caspase-3 activities, determined by cellular caspase-3 activity assay. $^{*}P<0.05$ versus Ctl; $^{\Phi}P<0.05$ versus *miR-605* alone; $n=5$ for each group. (**E**) Effects of nutlin-3 (3 μM) on miR-605 level in $p53^{+/+}$ HCT116 cells as compared with those in $p53^{-/-}$ HCT116 cells. Note that nutlin-3 is able to upregulate both *miR-605* and *miR-34a* only in $p53^{+/+}$ HCT116 cells. $^{*}P<0.05$ versus Ctl; $^{\Phi}P<0.05$ versus *miR-605* alone; $n=3$ for each group.

In summary, we have demonstrated here that (1) *miR-605* post-transcriptionally represses Mdm2; (2) *miR-605* is

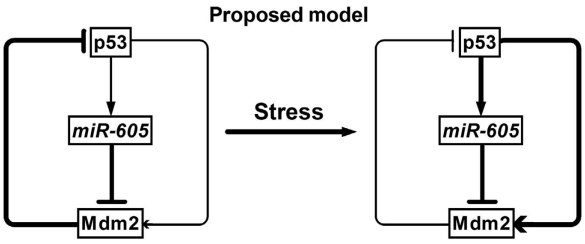

Figure 6 A proposed model describing the participation of *miR-605* to create a positive feedback loop that helps p53 escape the p53:Mdm2 negative feedback loop. The thickness of the lines indicates the strength of actions. In response to cellular stress, *miR-605* expression is enhanced due to initial p53 activation and this *miR-605* upregulation then feeds back to increase the transactivation activity of p53 by repressing Mdm2 to relieve the inhibitory effects of Mdm2 on p53.

transcriptionally activated by p53; (3) activation of p53 stimulates *miR-605* expression and *vice versa* overexpression of *miR-605* increases the transactivation activity of p53 resulting in upregulation of *miR-34a*; (4) inhibition of Mdm2 function upregulates both *miR-605* and *miR-34a* expression; and (5) *miR-605* preferentially induces cell death in WT p53-expressing cells.

Together with all these results, it appears that *miR-605* is able to disrupt p53:Mdm2 interaction similar to, but distinct from, a DNA-damaging agent or an Mdm2 inhibitor. DNA-damaging drugs activate p53 that in turn transcriptionally promotes Mdm2 expression. Mdm2 inhibitors bind to Mdm2 without changing Mdm2 level directly but increasing Mdm2 expression indirectly through releasing p53 from p53:Mdm2 interaction. By comparison, *miR-605* represses Mdm2 expression without directly affecting p53, and this repression relieves the inhibitory effect of Mdm2 on p53 leading to an indirect increase in p53 activity and expression that then further enhances *miR-605* expression. In this way, the participation of *miR-605* creates a positive feedback loop that helps p53 escape the p53:Mdm2 negative feedback loop (Figure 6).

p53 is at the centre of a complex molecular network regulating diverse physiological responses to cancer-related stresses. Activated p53 in response to DNA damage or oncogene activation induces cell cycle arrest, which can be transient or permanent (senescence), or promotes apoptosis in cases where the damage is too severe. The Mdm2 oncoprotein is a primary regulator of p53, mediating p53 control via ubiquitin-dependent proteasomal degradation. Activation of p53 in tumour cells by inhibiting its physical interaction with Mdm2 has been in the focus of cancer drug discovery (Dickens *et al*, 2010; Wade *et al*, 2010; Weber, 2010). Our study herein revealed that *miR-605* is a new component in the p53 gene network, serving as an on-and-off switch between the p53:Mdm2 negative feedback loop and the p53:*miR-605*:Mdm2 positive feedback loop. In response to cellular stresses, *miR-605* expression is enhanced due to initial p53 activation and this elevated *miR-605* level subsequently feeds back to increase the transactivation activity of p53 by repressing Mdm2 to relieve the inhibitory effects of Mdm2 on p53. Through this positive feedback loop, *miR-605* is able to aid rapid accumulation of p53 to induce cell cycle arrest or apoptosis. It appears that *miR-605* participates in the p53 signalling network differently from *miR-34a* though both are downstream transcriptional targets of p53. *miR-34a* is known to mediate the cellular function of p53 to regulate cell cycle progression, cellular senescence and apoptosis by targeting its downstream genes (Chang *et al*, 2007; Raver-Shapira *et al*, 2007; Welch *et al*, 2007; Rokhlin *et al*, 2008; Hermeking, 2010). By comparison, *miR-605* seems not to be directly involved in the cellular function of p53; rather it only acts to facilitate the function of p53 by enhancing the transactivation activity through inhibiting Mdm2. The data that AMO-34a is able to mitigate the apoptosis-promoting effects of *miR-605* but AMO-605 failed to affect the proapoptotic action of *miR-34a* (Figure 5C), plus the partial reversal of effect of *miR-605* by AMO-605, provides a strong evidence. In other words, *miR-605* itself is unable to induce apoptosis in the absence of p53 activation; this is supported by the results shown in Figure 5A and B that *miR-605* failed to induce apoptosis when p53 function was inhibited. Our findings therefore revealed that in addition to mediate the cellular function of p53 like the *miR-34* family, miRNAs, like *miR-605*, could also act to fine tune or amplify the activity of p53 to enhance its cellular function.

It should be noted, however, that we could not draw a conclusion from the present study as to whether the p53–*miR-605*–Mdm2 feedback signalling loop exists in other cell types neither could we draw a notion on what physiological role this pathway may have under *in vivo* conditions. Nonetheless, this study unraveled a novel molecular mechanism for fine tuning the dynamic shift of the p53 signalling network to favour or disfavour the function of p53 on demand, laying the groundwork for future studies on the implications of this type p53–miRNA interaction.

Materials and methods

Cell culture

Human breast cancer cells line MCF-7 with functional p53 status and MDA-MB-436 with non-functional mutant p53 (Lacroix and Leclercq, 2004; Keimling and Wiesmüller, 2009), human lung cancer cell line A549 (WT p53), the p53-null human lung adenocarcinoma cancer cell line H1299 used in this study was purchased from American Type Culture Collection (ATCC, Manassas, VA) and cultured in Dulbecco's Modified Eagle Medium or in RPMI 1640 supplemented with 10% FCS. Isogenic colorectal carcinoma HCT116 cells with or without p53 expression ($p53^{+/+}$ and $p53^{-/-}$, respectively) were gracefully provided by Dr Bert Vogelstein (The Howard Hughes Medical Institute and The Johns Hopkins Oncology Center, Baltimore, MD) (Bunz *et al*, 1998; Ericson *et al*, 2010).

Quantitative real-time RT–PCR analysis

The *mir*Vana™ qRT–PCR miRNA Detection Kit (Ambion) was used in conjunction with TaqMan real-time PCR for quantification of miRNAs in our study, as previously described in detail (Xiao *et al*, 2007; Yang *et al*, 2007; Luo *et al*, 2008). Total RNA samples were isolated from various cell lines with Ambion's *mir*Vana miRNA Isolation Kit and mRNA samples from various human tissues were purchased from Ambion. Reactions contained *mir*Vana qRT–PCR primer sets specific for human, rat and mouse *miR-605*, and for TP53 and Mdm2 were supplied by ABI. qRT–PCR was performed on a thermocycler ABI Prism® 7500 fast (Applied Biosystems) for 40 cycles. Fold variations in expression of an mRNA between RNA samples were calculated.

Western blot analysis

The cytosolic protein samples were extracted 48 h after treatments with the procedures essentially the same as described in detail elsewhere (Xiao *et al*, 2007; Yang *et al*, 2007; Luo *et al*, 2008). The

protein content was determined by BCA Protein Assay Kit using bovine serum albumin as the standard. Protein sample (~50 μg) was fractionated by SDS–PAGE (12% polyacrylamide gels) and transferred to PVDF membrane (Millipore, Bedford, MA). The sample was incubated overnight at 4°C with the primary antibodies in 1:200. Affinity purified rabbit polyclonal anti-p53 (mAb421; Enzo Life Sciences) and anti-Mdm2 antibodies (Cell Signaling) were used as the primary antibodies. Other primary antibodies (the antibodies to NFAT, IgG and lamin A) were all purchased from Santa Cruz Biotech. Next day, the membrane was incubated with secondary antibodies (Molecular Probes) diluted in PBS for 2 h at room temperature. Finally, the membrane was rinsed with PBS before scanning using the Infrared Imaging System (LI-COR Biosciences). Anti-GAPDH and anti-α-acting antibodies were used as internal controls for equal input of protein samples from cancer cell lines and from cardiac preparations, respectively. Western blot bands were quantified using QuantityOne software by measuring the band intensity (Area × OD) for each group and normalizing to GAPDH or α-acting. The final results are expressed as fold changes by normalizing the data to the control values.

Synthesis of miRNAs and anti-miRNA antisense inhibitors

miR-605 (5′-UAAAUCCCAUGGUGCCUUCUCCU-3′) and its antisense oligoribonucleotide fragment (AMO-605: 3′-AUUUAGGGUACCACG GAAGAGGA-5′) were synthesized by Integrated DNA Technologies Inc (IDT, Coralville, IA). Five nucleotides or deoxynucleotides at both ends of the antisense molecules were locked (the ribose ring is constrained by a methylene bridge between the 2′-*O*- and the 4′-C atoms). Additionally, a scrambled RNA was used as negative control; sense: 5′-UUCUCCGAACGUGUCACGUTT-3′ and antisense: 5′-ACGGACACGUUCGGAGAATT-3′ (Xiao *et al*, 2007; Yang *et al*, 2007; Luo *et al*, 2008).

Construction of luciferase—miRNA-target site fusion plasmids

To construct reporter vectors bearing miRNA-target sites, we synthesized the 3′UTR of *miR-605* target gene *Mdm2*, or the 3′UTR of TP53, by PCR amplification. The sense and antisense strands of the oligonucleotides were annealed by adding 2 μg of each oligonucleotides to 46 μl of annealing solution (100 mM K-acetate, 30 mM HEPES-KOH, pH 7.4 and 2 mM Mg-acetate) and incubated at 90°C for 5 min and then at 37°C for 1 h. The annealed oligonucleotides were digested with *Hin*dIII and *Spe*I. These inserts were ligated into *Hin*dIII and *Spe*I sites in the pMIR-REPORT luciferase miRNA expression reporter vector (Ambion) (Lin *et al*, 2007; Xiao *et al*, 2007; Yang *et al*, 2007; Luo *et al*, 2008).

Construction of PRKG1 promoter—luciferase fusion plasmids

A fragment (2861-AAAGTTCTTTCAGCTGTAATATACTATGACATGTT TTTTAATAATTCAGTGTTTATTCTTCTACCAGCATGTCTTTTCTCAAG CTTTCCTTGTGGTCTAA-2960) containing the three putative p53-binding motifs upstream the cGMP-dependent protein kinase 1, β-isozyme (PRKG1, the host gene of the intronic *miR-605*) was synthesized by Invitrogen. The fragment was then used as a template for PCR amplification with 5′-GGGGTACCAAAGTTCTTT CAGCTGTA-3′ and 5′-CCGCTCGAGTTAGACCACAAGGAAAGC-3′ as forward and reverse primers, respectively, using PCR Advantage and Advantage-GC genomic polymerase mixes (Clontech). The PCR product was subcloned into luciferase-containing pGL-3-Basic (Promega) vector, as described elsewhere (Lin *et al*, 2007). The integrity and orientation of all constructs were confirmed by restriction endonuclease analysis and DNA sequencing.

Preparation of decoy ODNs

Single-stranded phosphorothioate decoy ODNs were synthesized by IDT (Gao *et al*, 2006). The ODN was washed in 70% ethanol, dried and dissolved in sterilized Tris–EDTA buffer (10 mM Tris + 1 mM EDTA). The supernatant was purified using Micro Bio-spin30 columns (Bio-Rad, Hercules, CA) and quantified by spectrophotometry. The double-stranded decoy ODN was then prepared by annealing complementary single-stranded ODN by heating to 95°C for 10 min followed by cooling to room temperature slowly over 2 h. The decoy ODN was prepared at a concentration of 50 μM in saline. The sequence of p53 decoy ODN is sense 5′-AGA**CATG**CCTAGA **CATG**CCT-3′ and antisense 5′-TCTGTACGGATCTGTACGGA-3′ (The consensus core sequence is bold and underlined). For negative control, a mutant decoy ODN was also used: sense 5′-AGA**tgcaaa** TAGA**tgcaaa**T-3′ and antisense 5′-TCT**gacgtg**ATCT**acgtgg**A-3′. Nucleotide-substitution mutations to p53 decoy ODN were made using PCR-based methods.

Electrophoresis mobility shift assay

EMSA was performed with the digoxigenin (DIG) Gel Shift kit (Roche, Mannheim, Germany), as described previously (Gao *et al*, 2006; Lin *et al*, 2007). Varying amounts of nuclear protein extracts from MCF-7 cells were incubated with DIG-labelled double-stranded oligonucleotides containing the putative p53 *cis*-element from the PRGK1 promoter. For competition experiments, 100-fold excess of unlabelled double-stranded p53 consensus oligonucleotides, and for supershift experiments, 1 μg of p53 antibody (Cell Signaling), were added to the reaction. The generated chemiluminescent signals were recorded on the X-ray film. The sequences of the p53 *cis*-element examined are GTTTATTCTTCTACCAGCATGTCTTTTC TC; and the mutant p53 *cis*-element are GTTTATTCTTCTACCAG**tcgc** TCTTTTCTC (the replaced nucleotides are indicated by lower case letters.

Chromatin immunoprecipitation assay

ChIP assays were conducted with the EZ ChIP kit according to the manufacturer's instructions (Upstate Cell Signaling Solutions, Lake Placid, NY) (Lin *et al*, 2007). Briefly, MCF-7 cells were grown to subconfluency, washed and fixed in 1% formaldehyde for 10 min to crosslink nucleoprotein complexes and scraped in phosphate-buffered saline containing protease inhibitor cocktail. Pelleted cells were then lysed and sonicated in detergent lysis buffer. Sheared DNA–protein complexes were immunoprecipitated by incubating overnight the lysates with 2 μg antibodies against p53 or lamin A (as a control). Protein A/G Plus beads (Santa Cruz) were used, and after extensive washing, crosslinks were removed at 65°C over overnight in an elution buffer (1% SDS, 0.1 M $NaHCO_3$). The DNA was isolated using the QIAquick PCR purification kit (Qiagen) and the presence of the PRKG1 (the host gene of the intronic *miR-605*) promoter or of the p21 promoter as a positive control was analysed by PCR amplification using 10% of purified DNA. The primers used for the PRKG1 promoter sequence containing p53 *cis*-elements were 5′-GAGACCCTCACTCAGACGCA-3′ (forward) and 5′-CAGCACTAG GCTTCGGGTGG-3′ (reverse). The primers used for the p21 promoter sequence containing p53 *cis*-elements were from 5′-GA GCCTCCCTCCATCCCTATG-3′ (forward) and 5′-CTCCCAGCACACAC TCACAC-3′ (reverse). The PCR products were analysed by gel electrophoreses on an 8% non-denaturing polyacrylamide gel and subsequent ethidium bromide staining.

p53 overexpression and knockdown

To overexpress p53 or dominant-negative p53, the plasmids contained in the p53 Dominant-Negative Vector Set (Clontech) were transiently transfected into H1299 cells using lipofectamine 2000 reagent. p53 siRNA and Mdm2 siRNA, used to knockdown endogenous p53 and Mdm2, respectively, were purchased from Santa Cruz Biotech.

Transfection procedures

Cell lines or neonatal rat ventricular myocytes were transfected with a final concentration of 10 nM of *miR-605* and/or 5 nM of AMO-605, and negative control miRNAs or AMOs with lipofectamine 2000 (Invitrogen), according to the manufacturer's instructions. Forty-eight hours after transfection, cells were used for luciferase assay or were collected for total RNA or protein purification.

For decoy ODNs, cells were washed with serum-free medium once and then incubated with 50 μl fresh fetal bovine serum (FBS)-free medium. Decoy ODNs and lipofectamine 2000 (0.25 μl, Invitrogen, Carlsbad, CA) were separately mixed with 25 μl of Opti-MEM® I Reduced Serum Medium (Gibco, Grand Island, NY) for 5 min. Then, the two mixtures were combined and incubated for 20 min at RT. The lipofectamine:ODNs mixture was added dropwise to the cells and incubated at 37°C for 5 h. Subsequently, 25 μl fresh medium containing 30% FBS was added to the well and the cells were maintained in the culture until use.

Luciferase activity assay

For luciferase assay involving miRNA function, cells were transfected with the pMIR-REPORT luciferase miRNA expression reporter vector carrying the 3′UTR of *miR-605* target genes (Lin *et al*, 2007; Xiao *et al*, 2007; Yang *et al*, 2007; Luo *et al*, 2008).

For luciferase assay involving analysis of promoter activities of the *miR-605* host gene PRKG1, MCF-7 cells were simultaneously transfected with 10 nM *miR-605*, 1 μg PGL-3-target DNA (firefly luciferase vector) and 0.1 μg PRL-TK (TK-driven Renilla luciferase expression vector) with lipofectamine 2000. Following transfection (48 h), luciferase activities were measured with a dual luciferase reporter assay kit (Promega) on a luminometer (Lumat LB9507). For all experiments, transfection took place 24 h after starvation of cells in serum-free medium.

MTT assay for cell viability

Cell Proliferation Kit I (3-(4,5-dimethylthiazol-2-yl)-2,5-diphenyl tetrazolium bromide (MTT); Roche Molecular Biochemicals, Laval, PQ, Canada) was used to quantify surviving cells from oxidative stress, as previously described in detail (Xu *et al*, 2007; Lu *et al*, 2009).

Enzyme-linked immunosorbent assay (ELISA)

The Cell Death Detection ELISA kit (Roche Molecular Biochemicals) was employed to quantify DNA fragmentation on the basis of antibody detection of free histone and fragmented DNA, as detailed elsewhere (Gao *et al*, 2006; Xu *et al*, 2007; Lu *et al*, 2009).

Assays for caspase-3

The procedures for the assay for cellular caspase-3 activities have been previously described in detail elsewhere (Han *et al*, 2001). Briefly, after experimental treatment, cells were centrifuged (1000 *g*, 4°C, 10 min) and lysed. Sample was centrifuged at 10 000 *g* (4°C, 10 min), and the supernatant (10 μl) was incubated with 10 μl of substrate (2 mM Ac-DEVDpNA) in 80 μl of assay buffer at 37°C. Absorbance at 405 nm was read at several time points until readings reached plateau levels. Optical density changes relative to zero-time values were obtained as a measure of enzyme activity.

Terminal deoxyribonucleotide transferase-mediated dUTP nick end labelling (TUNEL)

DNA fragmentation of individual cells was detected with the *In Situ* Cell Death Detection kit, Fluorescein (Roche Molecular Biochemicals), as detailed previously (Han *et al*, 2001; Wang *et al*, 2002). TUNEL staining was analysed with a confocal microscope (Zeiss).

Data analysis

Group data are expressed as mean ± s.e.m. Statistical comparisons among multiple groups were performed by analysis of variance (ANOVA). If significant effects were indicated by ANOVA, a *t*-test with Bonferroni correction or a Dunnett's test was used to evaluate the significance of differences between individual means. Otherwise, baseline and drug data were compared by paired Student's *t*-test and age-matched comparisons between control and treatment were done by unpaired Student's *t*-test. Group comparisons for AF incidence were performed using χ^2-test. A two-tailed $P<0.05$ was taken to indicate a statistically significant difference.

miRNA (*miR-605* and *miR-214*) target gene was predicted using miRBase and *cis*-elements for transcription factor binding sites were analysed with *MatInspector* V2.2 (Genomatix).

Supplementary data

Supplementary data are available at *The EMBO Journal* Online (http://www.embojournal.org).

Acknowledgements

We thank XiaoFan Yang and Huizhen Wang for their excellent technical supports. This work was supported by the Canadian Institute of Health Research and Fonds de la Recherche de l'Institut de Cardiologie de Montreal.

Author contributions: Zhiguo Wang generated the hypothesis for this study, provided overall direction and supervision on the project, and wrote the manuscript; Jiening Xiao is the primary investigator who coordinated and designed the study and performed experiments and data analyses on luciferase, western blot and cell death; Huixian Lin is the second primary investigator involving every aspect of the study being responsible for characterizing the promoter region of *miR-605* gene subcloning; and Xiaobin Luo and Xiaoyan Luo contributed to the western blot analysis and qRT–PCR measurements.

Conflict of interest

The authors declare that they have no conflict of interest.

References

Barak Y, Juven T, Haffner R, Oren M (1993) mdm2 expression is induced by wild type p53 activity. *EMBO J* **12:** 461–468

Bunz F, Dutriaux A, Lengauer C, Waldman T, Zhou S, Brown JP, Sedivy JM, Kinzler KW, Vogelstein B (1998) Requirement for p53 and p21 to sustain G2 arrest after DNA damage. *Science* **282:** 1497–1501

Chang TC, Wentzel EA, Kent OA, Ramachandran K, Mullendore M, Lee KH, Feldmann G, Yamakuchi M, Ferlito M, Lowenstein CJ, Arking DE, Beer MA, Maitra A, Mendell JT (2007) Transactivation of miR-34a by p53 broadly influences gene expression and promotes apoptosis. *Mol Cell* **26:** 745–752

Dickens MP, Fitzgerald R, Fischer PM (2010) Small-molecule inhibitors of MDM2 as new anticancer therapeutics. *Semin Cancer Biol* **20:** 10–18

Eischen CM, Lozano G (2009) p53 and MDM2: antagonists or partners in crime? *Cancer Cell* **15:** 161–162

Ericson K, Gan C, Cheong I, Rago C, Samuels Y, Velculescu VE, Kinzler KW, Huso DL, Vogelstein B, Papadopoulos N (2010) Genetic inactivation of AKT1, AKT2, and PDPK1 in human colorectal cancer cells clarifies their roles in tumor growth regulation. *Proc Natl Acad Sci USA* **107:** 2598–2603

Gao H, Xiao J, Yang B, Sun Q, Lin H, Bai Y, Yang L, Wang H, Wang Z (2006) A single decoy oligodeoxynucleotides targeting multiple oncoproteins produces strong anti-cancer effects. *Mol Pharmacol* **70:** 1621–1629

Han H, Wang H, Long H, Nattel S, Wang Z (2001) Oxidative preconditioning and apoptosis in L-cells: roles of protein kinase B and mitogen-activated protein kinases. *J Biol Chem* **276:** 26357–26364

Harris SL, Levine AJ (2005) The p53 pathway: positive and negative feedback loops. *Oncogene* **24:** 2899–2908

Haupt Y, Maya R, Kazaz A, Oren M (1997) Mdm2 promotes the rapid degradation of p53. *Nature* **387:** 296–299

He L, He X, Lim LP, de Stanchina E, Xuan Z, Liang Y, Xue W, Zender L, Magnus J, Ridzon D, Jackson AL, Linsley PS, Chen C, Lowe SW, Cleary MA, Hannon GJ (2007) A microRNA component of the p53 tumour suppressor network. *Nature* **447:** 1130–1134

Hermeking H (2010) The miR-34 family in cancer and apoptosis. *Cell Death Differ* **17:** 193–199

Honda R, Tanaka H, Yasuda H (1997) Oncoprotein MDM2 is a ubiquitin ligase E3 for tumor suppressor p53. *FEBS Lett* **420:** 25–27

Keimling M, Wiesmüller L (2009) DNA double-strand break repair activities in mammary epithelial cells––influence of endogenous p53 variants. *Carcinogenesis* **30:** 1260–1268

Kubbutat MH, Jones SN, Vousden KH (1997) Regulation of p53 stability by Mdm2. *Nature* **387:** 299–303

Lacroix M, Leclercq G (2004) Relevance of breast cancer cell lines as models for breast tumours: an update. *Breast Cancer Res Treat* **83:** 249–289

Lee I, Ajay SS, Yook JI, Kim HS, Hong SH, Kim NH, Dhanasekaran SM, Chinnaiyan AM, Athey BD (2009) New class of microRNA targets containing simultaneous 5′-UTR and 3′-UTR interaction sites. *Genome Res* **19:** 1175–1183

Lin H, Xiao J, Luo X, Xu C, Gao H, Wang H, Yang B, Wang Z (2007) Overexpression HERG K^+ channel gene mediates cell-growth signals on activation of oncoproteins Sp1 and NF-κB and inactivation of tumor suppressor Nkx3.1. *J Cell Physiol* **212:** 137–147

Lu Y, Xiao J, Lin H, Bai Y, Luo X, Wang Z, Yang B (2009) Complex antisense inhibitors offer a superior approach for microRNA research and therapy. *Nucleic Acids Res* **37:** e24–e33

Luo X, Lin H, Pan Z, Xiao J, Zhang Y, Lu Y, Yang B, Wang Z (2008) Overexpression of Sp1 and downregulation of miR-1/miR-133 activates re-expression of pacemaker channel genes HCN2 and HCN4 in hypertrophic heart. *J Biol Chem* **283:** 20045–20052

Momand J, Zambetti GP, Olson DC, George D, Levine AJ (1992) The mdm-2 oncogene product forms a complex with the p53 protein and inhibits p53-mediated transactivation. *Cell* **69:** 1237–1245

Morishita R, Sugimoto T, Aoki M, Kida I, Tomita N, Moriguchi A, Maeda K, Sawa Y, Kaneda Y, Higaki J, Ogihara T (1997) *In vivo* transfection of cis element 'decoy' against nuclear factor-kappaB binding site prevents myocardial infarction. *Nat Med* **13:** 894–899

Raver-Shapira N, Marciano E, Meiri E, Spector Y, Rosenfeld N, Moskovits N, Bentwich Z, Oren M (2007) Transcriptional activation of miR-34a contributes to p53-mediated apoptosis. *Mol Cell* **26:** 731–743

Rokhlin OW, Scheinker VS, Taghiyev AF, Bumcrot D, Glover RA, Cohen MB (2008) MicroRNA-34 mediates AR-dependent p53-induced apoptosis in prostate cancer. *Cancer Biol Ther* **7:** 1288–1296

Shangary S, Wang S (2009) Small-molecule inhibitors of the MDM2-p53 protein-protein interaction to reactivate p53 function: a novel approach for cancer therapy. *Annu Rev Pharmacol Toxicol* **49:** 223–241

Tarasov V, Jung P, Verdoodt B, Lodygin D, Epanchintsev A, Menssen A, Meister G, Hermeking H (2007) Differential regulation of microRNAs by p53 revealed by massively parallel sequencing: miR-34a is a p53 target that induces apoptosis and G1-arrest. *Cell Cycle* **6:** 1586–1593

Vassilev LT (2007) MDM2 inhibitors for cancer therapy. *Trends Mol Med* **13:** 23–31

Wade M, Wang YV, Wahl GM (2010) The p53 orchestra: Mdm2 and Mdmx set the tone. *Trends Cell Biol* **20:** 299–309

Wang H, Zhang Y, Cao L, Han H, Wang J, Yang B, Nattel S, Wang Z (2002) HERG K^+ channel: a regulator of tumor cell apoptosis and proliferation. *Cancer Res* **62:** 4843–4848

Weber L (2010) Patented inhibitors of p53-Mdm2 interaction (2006–2008). *Expert Opin Ther Pat* **20:** 179–191

Welch C, Chen Y, Stallings RL (2007) MicroRNA-34a functions as a potential tumor suppressor by inducing apoptosis in neuroblastoma cells. *Oncogene* **26:** 5017–5022

Xiao J, Luo X, Lin H, Zhang Y, Lu Y, Wang N, Zhang Y, Yang B, Wang Z (2007) MicroRNA miR-133 represses HERG K^+ channel expression contributing to QT prolongation in diabetic hearts. *J Biol Chem* **282:** 12363–12367

Xu C, Lu Y, Lin H, Xiao J, Wang H, Luo X, Li B, Wang Z, Yang B (2007) The muscle-specific microRNAs miR-1 and miR-133 produce opposing effects on apoptosis via targeting HSP60/HSP70 and caspase-9 in cardiomyocytes. *J Cell Sci* **120:** 3045–3052

Yang B, Lin H, Xiao J, Lu Y, Luo X, Li B, Zhang Y, Xu C, Bai Y, Wang H, Chen G, Wang Z (2007) The muscle-specific microRNA miR-1 causes cardiac arrhythmias by targeting GJA1 and KCNJ2 genes. *Nat Med* **13:** 486–491

